Theor Appl Climatol (2012) 109:635–643
DOI 10.1007/s00704-012-0600-7

ORIGINAL PAPER

Three-dimensional air–sea interactions investigated with bilayer networks

Aixia Feng · Zhiqiang Gong · Qiguang Wang · Guolin Feng

Received: 18 August 2011 / Accepted: 3 February 2012 / Published online: 25 February 2012

Abstract We introduce bilayer networks in this paper to study the coupled air–sea systems. Results show that the framework of bilayer networks is powerful for studying the statistical topology structure and dynamics in the fields of ocean and atmosphere. Based on bilayer networks, the inner and cross interactions of the sea surface temperature (SST) field and the height field are displayed, and the main three-dimensional air–sea interaction pattern is identified. The formation of the main pattern can be explained by the "gearing between the Indian and Pacific Ocean (GIP)" model; therefore, the pattern existence can be confirmed reliably. Furthermore, lead–lag analysis reveals the trigger processes of the "GIP". That is, the anomalies of the tropical mid-eastern Pacific Ocean SST (TMEPO-SST) appear first; then, through the Walker circulation, the 850-hPa geopotential height over the Pacific Islands responds to the anomalies of the TMEPO-SST 2 months later; finally, the tropical Indian Ocean SST (TIO-SST) responds to the anomalies of the height 1 month later through the Asian monsoon circulation. Therefore, the impacts of the TMEPO-SST to the TIO-SST show 3 months later through the air–sea interactions between the components of the main three-dimensional air–sea interaction mode. The new framework uncovers already-known as well as other novel features of the air–sea systems and general circulation. The application of complex network theory and methodology to understand the complex interactions between the oceans and the atmosphere is promising.

A. Feng · Q. Wang
College of Atmospheric Sciences, Lanzhou University,
Lanzhou 730000, People's Republic of China
e-mail: fax20032008@gmail.com

Q. Wang
e-mail: photon316@163.com

A. Feng · Z. Gong · Q. Wang · G. Feng (✉)
Laboratory for Climate Studies, National Climate Center,
China Meteorological Administration,
Beijing 100081, People's Republic of China
e-mail: fax20032008@163.com

Z. Gong
e-mail: gzq0929@126.com

1 Introduction

The last fewer decades have witnessed the widespread application of complex networks to ecological, social, biological, and technological systems (Watts and Strogatz 1998; Albert and Barabasi 2002; Newman 2003). Most of these studies focus on the networks representation by one kind of node or interaction. However, it was realized that super-networks or networks of networks could be a more appropriate way to describe the complex systems. The dynamical structure of the whole network can be considered as interactions between and within subnetworks. The well-studied networks by the notation are the mammalian cortex networks (Zhou et al. 2006, 2007) and the infrastructure networks (Kurant and Thiran 2006; Kurant et al. 2007; Buldyrev et al. 2010; Parshani et al. 2010). In transportation networks, a layered model is introduced to describe the system, in which two network layers are used to represent the physical infrastructure and the traffic flows (Kurant and Thiran 2006; Kurant et al. 2007). Recently, interconnecting bilayer networks are proposed to study the wide range of empirical networks (Xu et al. 2011). These are important works for the further development of the complex systems.

The climate networks are also well-studied to reveal the spatio-temporal structures of the climatic variation and the mechanism of the climate dynamics over the globe or a region (Tsonis and Roebber 2004; Tsonis et al. 2006, 2008b; Gong et al. 2008; Wang and Tsonis 2008, 2009; Zhou et al. 2008, 2009, 2010; Donges et al. 2009a, b; Zou et al. 2011; Steinhaeuser et al. 2011). The works include studying of the role of teleconnections (Tsonis et al. 2008a),

Table 1 The linking probability of the air–sea coupled climate networks: the lower layer subnetwork refers to the SST field, and the upper layer subnetwork refers to the 850-hPa geopotential height field

Networks	Whole	Lower layer	Upper layer	Cross
Density	0.024	0.038	0.053	0.002

The edge density for the whole networks is the ratio connections of the total network nodes. That for the lower layer subnetwork is the ratio connections of the lower layer subnetwork nodes, and the similar definition for the upper layer edge density. The cross edge density is the ratio connections of the cross nodes

the impact of the El Niño and La Niña phenomena (Tsonis and Swanson 2008; Yamasaki et al. 2008; Gozolchiani et al. 2008), the climate shifts (Tsonis et al. 2007; Wang et al. 2008), and the climate extreme events (Wang et al. 2009) in the perspective of complex networks. Furthermore, the topological quantity of the climate networks is used to make prediction (Steinhaeuser et al. 2010). Among the works, coupled subnetworks are applied to study vertical topological structures of the geopotential height for understanding the circulation (Donges et al. 2011). In this paper, bilayer networks are applied to study the air–sea interactions, which is a fascinating, tough, and important issue in climate study. In the bilayer networks, the networks are divided into lower layer and upper layer subnetworks. In our study, the surface sea temperature is regarded as the lower layer subnetwork, and 850-hPa geopotential height level as the upper layer subnetwork. The air–sea systems can be studied by investigating the inner-layer and cross-layer characteristics to reveal their topological and dynamical structures.

2 Data and methodology

The data used here are the monthly averaged geopotential height of reanalysis data, with a latitude–longitude resolution of 5×5°, and the monthly averaged surface sea temperature (SST) from the NOAA of V3b with latitude–longitude resolution of 4×4°. The range of the latitudes is between 60°S and 60°N, so the grid points of geopotential height field and SST field are 1,880 and 2,790, respectively. For each grid point, monthly values are from January 1948 to December 2010. To minimize the bias introduced by the external solar forcing common to all time series in the data sets, we calculated the anomaly time series from the original ones. That is to remove the mean annual cycle by subtracting the climatological average for each month.

To study the coupled air–sea systems by complex networks, the grid points are assumed to be the nodes of the networks denoted by a node set $V=\{v_1,v_2,\cdots,v_N\}$, where N is the total number of the nodes. There are two variables in the networks; therefore, we divided the networks into two layer subnetworks. One layer subnetwork is referred to the nodes of the SST field and the connection relationships among them called lower layer subnetwork. The set of the lower layer nodes is denoted by $V_1=\{i_1,i_2,\cdots,i_{N_1}\}$, N_1=2,790, where i and N_1 represents the nodes and the total node number of the layer respectively. The other layer subnetwork is referred to the nodes of the 850-hPa geopotential height field and the connection relationships among them called upper layer subnetwork. Its node set is $V_2=\{j_1,j_2,\cdots,j_{N_2}\}$, N_2=1,880, and the symbols are similar to the lower layer subnetwork. By definition, we have $V_1\cup V_2=$

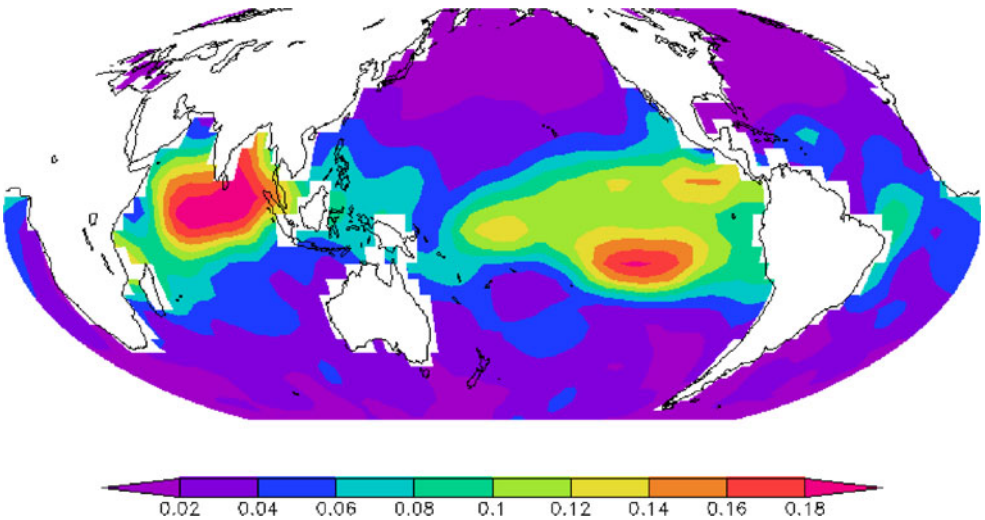

Fig. 1 The geographic distribution of the weighted node degree in the lower layer subnetwork

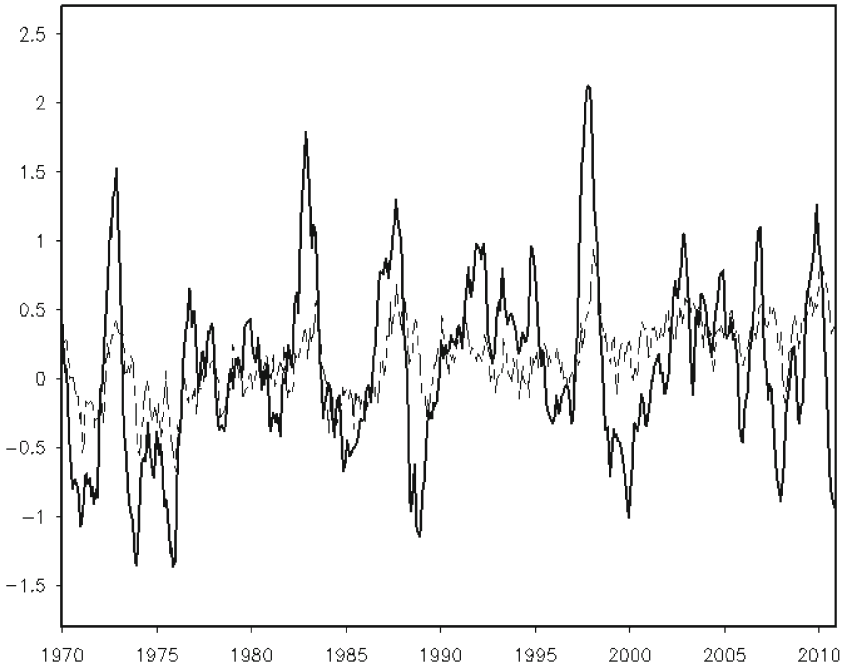

Fig. 2 The SST anomalies over the Pacific Ocean (8°S–8°N, 180–272°E, *the solid line*) and the Indian Ocean (8°S–8°N, 44°E–100°E, *the dashed line*) from 1971 to 2010

V and N=N_1+N_2. In order to introduce the links (i.e., their connection relationships) between nodes, the Pearson correlation coefficient r at non-lag between the anomaly time series of all possible pairs of nodes is calculated. A pair of nodes has an edge if their absolute value of correlation coefficient greater or equal to 0.5 (Tsonis and Swanson 2008). There exist three kinds of edges, the edges among the nodes of the lower layer subnetwork denoted by edge set $E_1 = \{e_1(ii), e_2(ii), \cdots, e_{M_1}(ii)\}$, the edges among the nodes of the upper layer subnetwork denoted by edge set $E_2 = \{e_1(jj), e_2(jj), \cdots, e_{M_2}(jj)\}$, and the edges connecting the two layer called cross edges denoted by edge set $E_{12} = \{e_1(ij), e_2(ij), \cdots, e_{M_{12}}(ij)\}$ (the nodes connecting the cross edges are called cross nodes), then $E_1 \cup E_2 \cup E_{12} = E$ and $M = M_1 + M_2 + M_{12}$, where E is the edge set of the whole networks, and M is the total number of the whole network edges. The density of the edges is defined as $\rho = \frac{2|M|}{N(N-1)}$ for the whole networks, thus $\rho_1 = \frac{2|M_1|}{N_1(N_1-1)}$ for the lower layer subnetwork, $\rho_2 = \frac{2|M_2|}{N_2(N_2-1)}$ for the upper layer subnetwork and $\rho_{12} = \frac{2|M_{12}|}{N_1 N_2}$ for the cross edges connecting the two subnetworks to measure the proportion that the nodes could be connected.

The node degree is a popular physical quantity to describe the topology property and centrality of the nodes. For the climate bilayer networks, we focused on the properties of the lower layer subnetwork, the upper layer subnetwork and the cross properties connecting the two subnetworks. The node degree of lower layer subnetwork, the upper layer subnetwork and the cross node degree (cross nodes mean connecting the other subnetwork nodes) are respectively defined as:

$$k_i^1 = \sum_{l\in V_1, l=1}^{l=N_1} a_{il}, k_j^2 = \sum_{l\in V_2, l=1}^{l=N_2} a_{jl}, k_i^{12} = \sum_{l\in V_2, l=1}^{l=N_2} a_{il}, k_j^{12} = \sum_{l\in V_1, l=1}^{l=N_1} a_{jl}. \quad (1)$$

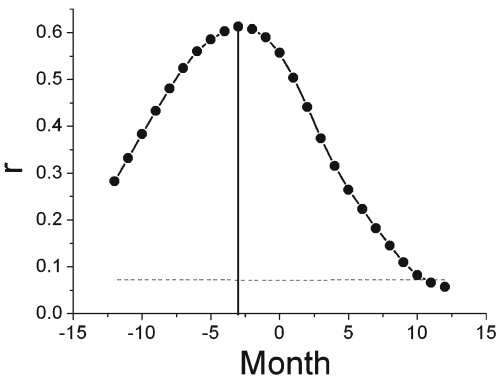

Fig. 3 The cross correlation (r) between the tropical mid-eastern Pacific Ocean and tropical Indian Ocean in the SST anomaly field with lags −12 month to 12 month (the Indian Ocean leading as the positive value). The *dashed line* is the 95% significance level, and the *vertical black line* shows the lead–lag month with the maximum cross correlation coefficient

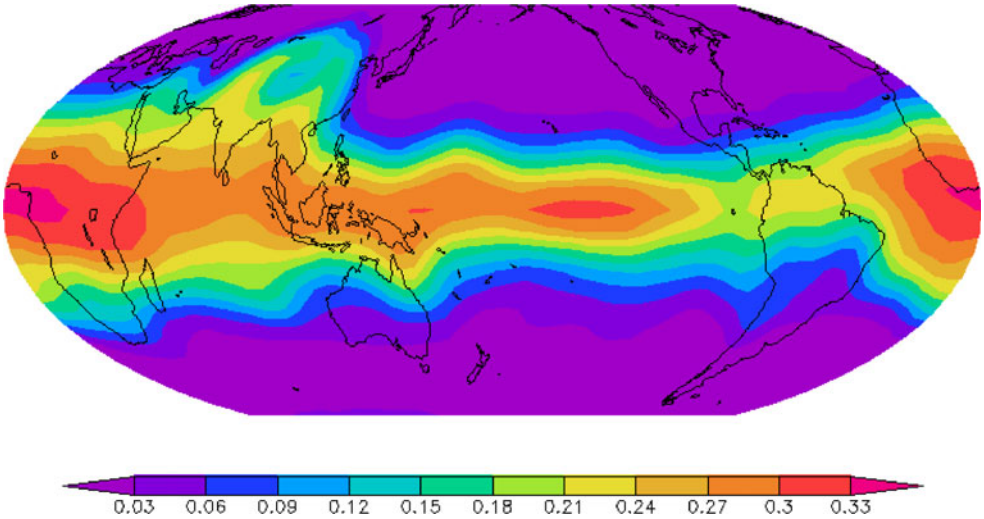

Fig. 4 The same as Fig. 1 but for the upper layer subnetwork

While the weighted degrees are:

$$w_i^1 = \frac{\sum_{l\in V_1, l=1}^{l=N_1} a_{il}\cos\phi_l}{\sum_{l\in V_1, l=1}^{l=N_1}\cos\phi_l}, w_j^2 = \frac{\sum_{l\in V_2, l=1}^{l=N_2} a_{jl}\cos\phi_l}{\sum_{l\in V_2, l=1}^{l=N_2}\cos\phi_l}, w_i^{12} = \frac{\sum_{l\in V_2, l=1}^{l=N_2} a_{il}\cos\phi_l}{\sum_{l\in V_2, l=1}^{l=N_2}\cos\phi_l}, w_j^{12} = \frac{\sum_{l\in V_1, l=1}^{l=N_1} a_{jl}\cos\phi_l}{\sum_{l\in V_1, l=1}^{l=N_1}\cos\phi_l}. \quad (2)$$

Where a_{il} or a_{jl} is the element of the adjacent matrix with a_{il} or a_{jl}=1 if there exists edge between i and l or j and l, otherwise a_{il}=0 or a_{jl}=0. The node degree measures the centrality of the node in the networks, and the weighted degree is the same but minimizing the bias induced by different grid points representing different area on the earth.

3 Results and discussion of the air–sea bilayer climate networks

The densities of the constructed bilayer climate networks are summarized in Table 1. The densities of the upper layer subnetwork and the lower layer subnetwork are almost identical, but the cross density is much smaller (about 1/20) than those of

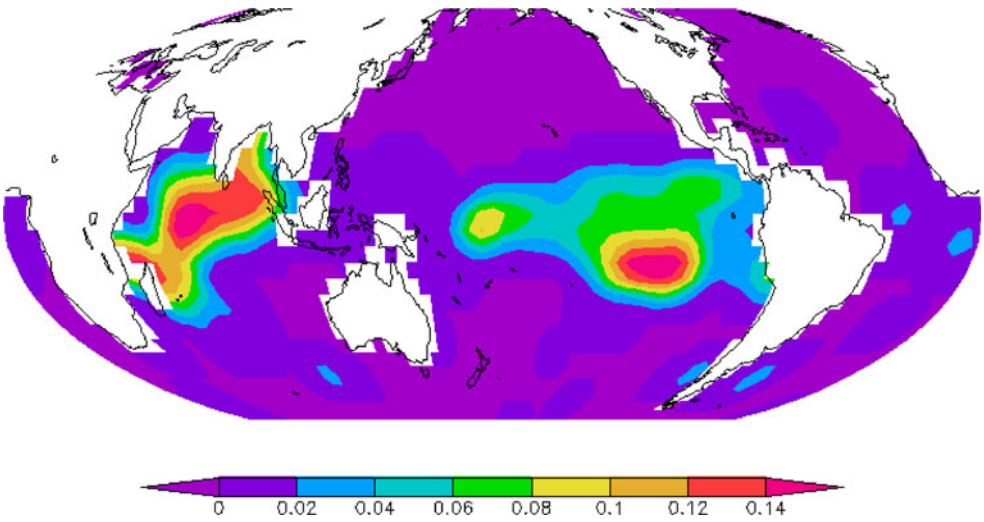

Fig. 5 The geographic distribution of the weighted cross node degree in the lower layer subnetwork

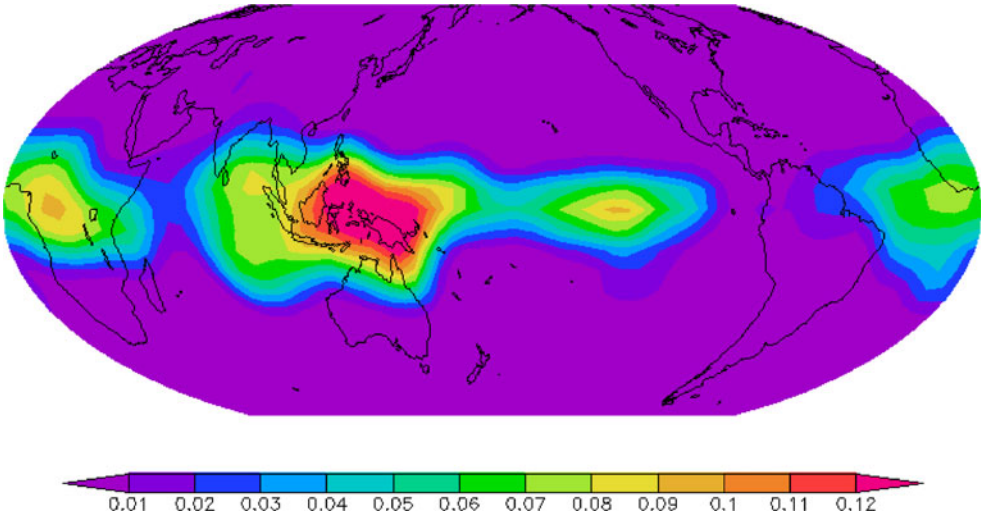

Fig. 6 The same as Fig. 5 but for the upper layer subnetwork

the two singular layer subnetworks. That is to say, there is physical separation between the SST field and 850-hPa geopotential height field on underlying dynamics. That is why we introduce bilayer networks to study the air–sea systems.

The weighted node degree of the lower layer subnetwork is color-contoured in Fig. 1. The spatial heterogeneity of the averaged linear correlation structure in SST field is clearly distinct. The weighted node degree is significantly larger in both the tropical Indian Ocean and the tropical mid-eastern Pacific Ocean than other ocean regions. They are key regions affecting the climatic systems. In order to identify the relationships between them, the non-lag SST anomaly evolution of the two oceans is illustrated by Fig. 2 (only the periods from 1971 to 2010 are displayed for clearness). It shows that SST variations in the two ocean regions are positive. The mean cross correlation coefficient of them is 0.56 from 1948 to 2010. That is rather larger than the value of 0.07 for statistically significant level 95%, and it has the highest value at lag −3 months just as Fig. 3 has shown. It reveals that the changes of the two oceans are consistent with each other, and the change of tropical mid-eastern Pacific Ocean SST (TMEPO-SST) leads that of the tropical Indian Ocean by 3 months. It is hard to explain the inner-process of the oceans because of the isolation of the two oceans by islands. The phenomenon will be explained later in the paper. The structure of weighted node degree in the upper layer subnetwork is shown in Fig. 4. Similar to the SST field, the 850-hPa geopotential height field also has a stronger correlation in the tropical regions than the mid–high latitudes. That implies the centrality role of the equatorial regions.

The weighted cross node degrees of the lower layer and upper layer subnetworks are illustrated in Figs. 5 and 6, respectively. The regions with largest weighted cross node degree are over the tropical mid-eastern Pacific Ocean and Indian Ocean in the SST field, and over the islands what separate the Indian Ocean from the Pacific Ocean in the tropics in the 850-hPa circulation field. It implies the

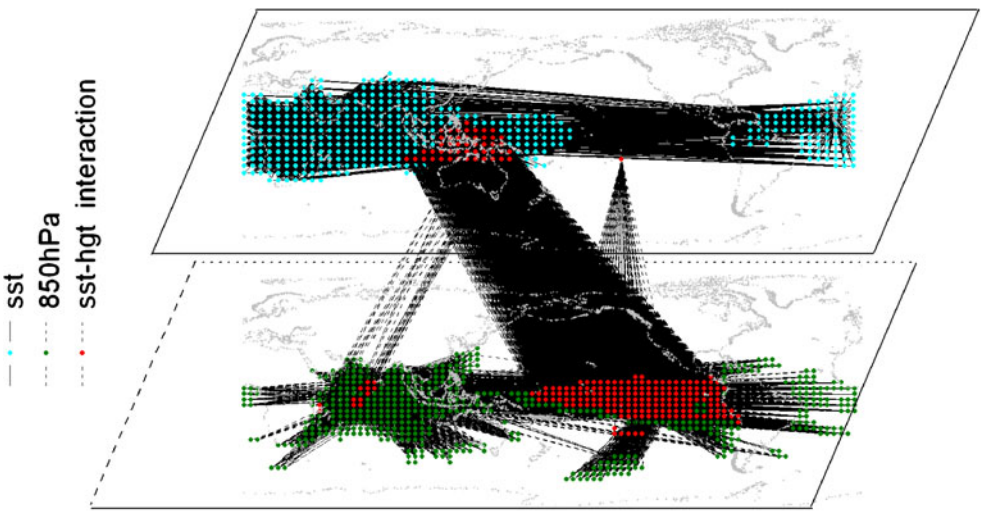

Fig. 7 The graph of bilayer air–sea interaction networks: the *dots with olive color* and *cyan color* represent the nodes with weighted node degree greater than 0.18 for the lower layer subnetwork and 0.14 for the upper layer subnetwork, respectively. The *red dots* represent the cross nodes with weighted node degree greater than 0.06. The *black dashes* or *solid lines* represent edges

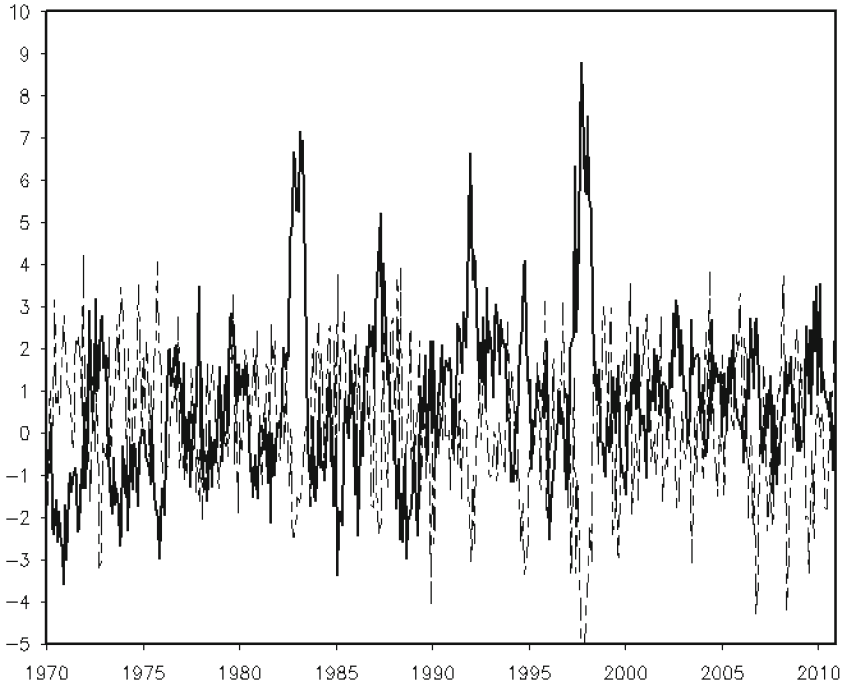

Fig. 8 The same as Fig. 2 but for the anomaly U-winds of 850 hPa over the two oceans

important role of the regions in the air–sea interaction process. The strong interactions of the bilayer networks are demonstrated in Fig. 7. It visualizes the three-D inner and cross interactions between the SST field and the height field. We call the correlation structure "the main three-D air–sea interaction pattern". In the lower layer, the correlation between the tropical Indian Ocean and mid-eastern Pacific Ocean is high. The two oceans are also correlated highly to the tropical Atlantic Ocean, the west Pacific Ocean, and the mid–high latitudes of southern Indian Ocean and southern Pacific Ocean. The pattern of the SST field inner-correlation is like irregular double stars and the central discs are the two tropical oceans. The shape of interactions for the 850 hPa looks like band centers over in the African continent, the tropical Indian Ocean, south of Eurasia, equatorial west Pacific Ocean and the tropical Atlantic Ocean. For "the main three-D air–sea interaction pattern", the main interactions are between the atmospheres over the tropical islands (Malayan Peninsula and Indonesian archipelago) and the sea in the Indian Ocean, and between the atmospheres over the tropical islands and the sea in the Pacific Ocean. Furthermore, the latter interactions are much closer. The non-lag correlation coefficients between the anomalous geopotential height over the islands area (12°S–8°N, 115°E–150°E, in 850 hPa) and the anomaly SST of the two oceans are 0.61 and 0.65, respectively.

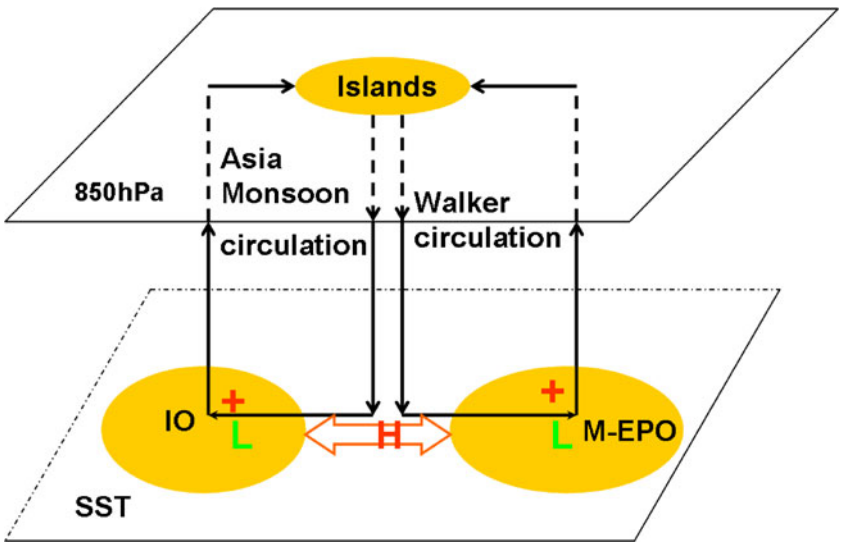

Fig. 9 Scheme of the air–sea interaction mechanism among the Indian Ocean (*IO*), the mid-eastern Pacific Ocean (*M-EPO*) and the lower tropospheric atmosphere (over the islands isolating the two oceans) when the SST anomalies are positive

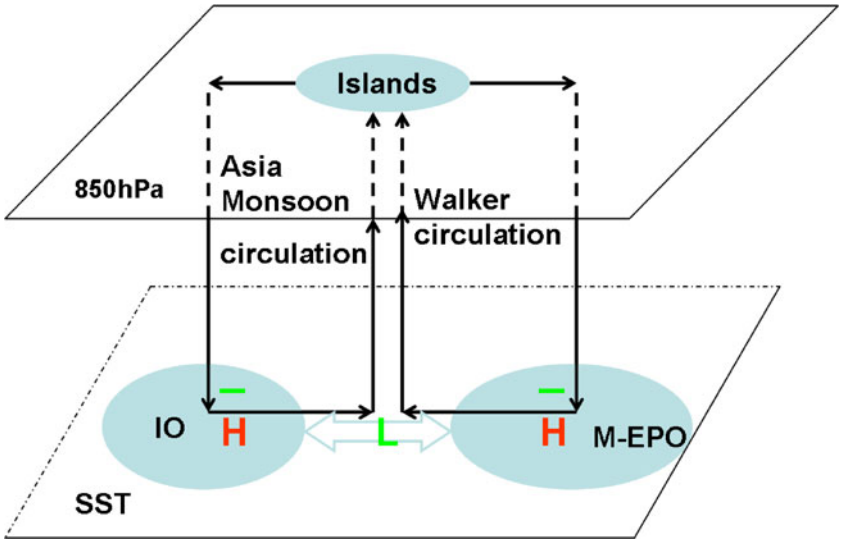

Fig. 10 The same as Fig. 9 but for the negative SST anomalies

The consistent variations between the components of "the main three-D air–sea interaction pattern" imply that the underlying dynamical mechanisms drive them connected closely. One explanation is possible that the SST changes over the two oceans and the geopotential height variations over the tropical islands are linked by the atmosphere circulation. The circulation cells over the oceans are the Asian monsoon circulation (over the Indian Ocean) and Walker circulation (over the Pacific Ocean). The U-wind anomaly changes of the two circulation cells with time are shown in Fig. 8. They are negatively correlated with the coefficient −0.31, and the value is higher than that of statistically significant level 95% as well. Therefore, the variations of the two circulation cells are consistent, but they are opposite in directions. The processes of air–sea interactions over the tropical Indian–Pacific Ocean regions can be illustrated by Figs. 9 and 10. When the SST anomalies of the two oceans are positive, the anomaly flows are upward over the oceans. Therefore, the sea level pressure over the oceans is relatively lower than the climatological state. Under the effect of U-wind of the Asian monsoon circulation and the Walker circulation, the upward flows mix with the U-winds and flow to the region over the tropical islands. After that, the flows subside, making the tropical islands surface pressure high. Because of the high pressure in the region, the surface flows are blown from the islands to the two oceans and forms the closure atmosphere circulations of the Asian monsoon circulation and Walker circulation, respectively. The Asian monsoon circulation is clockwise and the Walker circulation is counter-clockwise (Fig. 9). When the SST anomalies over the two tropical oceans are negative, the situation is opposite just as Fig. 10 illustrated. The mechanism is called the "GIP" model, which has successfully explained the significant positive correlation on SST anomalies between the equatorial Indian Ocean and the eastern equatorial Pacific Ocean (Wu and Meng 1998; Meng and Wu 2000). The model shows the coupled circulations working in a way like a pair of gears operating over the equatorial Indian Ocean and Pacific Ocean, and reveals the "gearing point" located at the Indonesia archipelago. Our "main three-dimensional air–sea interaction pattern" is just consistent with the model exhibits, i.e., the weighted node degree (a topological physical quantity of bilayer framework) spatial distribution. Apparently, the observation study here is rather simple than the numerical simulation of the climate models.

The lead–lag relationships are investigated between the key components of "the three-D air–sea interaction pattern" to detect the cause–effect among them. The TMEPO-SST anomalies lead the tropical islands 850-hPa geopotential height anomalies by 2 months. Nevertheless, the tropical islands 850-hPa geopotential height anomalies lead the tropical Indian SST anomalies by 1 month. That is to say, the anomalies begin at the TMEPO-SST first; then, the tropical islands 850-hPa geopotential height responds 2 months later through Walker circulation; finally, the tropical Indian

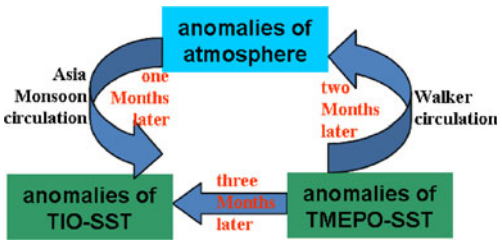

Fig. 11 Scheme for the trigger processes on air–sea system anomaly: TMEPO-SST and TIO-SST are the abbreviations of tropical mid-eastern Pacific Ocean SST and tropical Indian Ocean SST respectively, and the atmosphere here refer to the air over the tropical islands in 850-hPa geopotential height field

Ocean SST (TIO-SST) responds to the change of geopotential height 1 month later and to that of the tropical mid-eastern Pacific Ocean 3 months later, just as Fig. 11 shows. That is consistent with that in Fig. 3. In conclusion, the anomaly of the tropical mid-eastern Pacific Ocean leads the anomaly of the tropical Indian SST through the Asian monsoon circulation and Walker circulation by 3 months.

4 Conclusions

In summary, we introduce bilayer networks to study the air–sea interactions and investigate the characteristics of the coupled climate networks. The technique focuses on revealing the topological structure and dynamical mechanism of the air–sea systems. The spatial weighted node degree distribution of the bilayer networks reveals the correlation structures in the SST field, the 850-hPa geopotential height field and the interactions between them. The central regions of the correlation are located at tropical Indian Ocean and Pacific Ocean in the SST field, and tropics in the 850-hPa field. The main three-dimensional air–sea interaction pattern is identified over the two oceans in the SST field and over the islands what separate the Indian Ocean from Pacific Ocean in tropics in the 850-hPa field. The pattern formation is explained by the coupled Asian monsoon circulation and Walker circulation called "GIP" model. The lead–lag relationships of the pattern components reveal the trigger processes of the "GIP" that the SST anomaly of the tropical mid-eastern Pacific Ocean leads to the anomaly of the TIO-SST through the Asian monsoon circulation and Walker circulation, and the SST of the tropical Indian responds to the TMEPO-SST anomaly 3 months later. The facts prove that it is fruitful to apply bilayer networks to study the air–sea systems. Following the presentation mentioned above, we should say, the application of bilayer networks to study the air–sea systems is useful and perspective.

Acknowledgments We give our thanks to Professor A. A. Tsonis, H. X. Cao and D. R. He for constructive suggestions and revision of the paper. We also thank the editors and the reviewers for their insightful comments and helpful suggestions. This work is supported by the Chinese National Natural Science Foundation under grant number 40930952, the State Key Development Program for Basic Research under grant number 2012CB9955203.

References

Albert R, Barabasi A-L (2002) Statistical mechanics of complex networks. Rev Mod Phys 74:47–97. doi:10.1103/RevModPhys.74.47

Buldyrev SV, Parshani R, Paul G, Stanley HE, Havlin S (2010) Catastrophic cascade of failures in interdependent networks. Nature 464:1025–1028. doi:10.1038/nature089321

Donges JF, Zou Y, Marwan N, Kurths J (2009a) The backbone of the climate network. Europhys Lett 87:48007. doi:101209/0295-5075/87/48007

Donges JF, Zou Y, Marwan N, Kurths J (2009b) Complex networks in climate dynamics. Eur Phys J Special Topics 174:157–179. doi:101140/epjst/e2009-01098-2

Donges JF, Schultz HCH, Marwan N, Zou Y, Kurths J (2011) Investigating the topology of interacting networks: theory and application to coupled climate subnetworks. Eur Phys J B. doi:10.1140/epjb/e2011-10795-8

Gong ZQ, Zhou L, Zhi R, Feng GL (2008) Analysis of dynamical statistical characteristics of temperature correlation networks of 1-30D scales. Acta Phys Sin 57:5351–5360

Gozolchiani A, Yamasaki K, Gazit O, Havlin S (2008) Pattern of climate network blinking links follows El Niño events. Europhys Lett 83:28005. doi:101209/0295-5075/83/28005

Kurant M, Thiran P (2006) Layered complex networks. Phys Rev Lett 96:138701. doi:101103/PhysRevLett96138701

Kurant M, Thiran P, Hagmann P (2007) Error and attack tolerance of layered complex networks. Phys Rev E 76:026103. doi:101103/PhysRevE76026103

Meng W, Wu GX (2000) Gearing between the Indo-monsoon Circulation and the Pacific-Walker Circulation and the ENSO, part II: numerical simulation. Chin J Atmos Sci 24:15–25

Newman MEJ (2003) The structure and function of complex networks. SIAM Rev 45:167–256

Parshani R, Buldyrev SV, Havlin S (2010) Interdependent networks: reducing the coupling strength leads to a change from a first to second order percolation transition. Phys Rev Lett 105:048701. doi:101103/PhysRevLett105048701

Steinhaeuser K, Chawla NV, Ganguly AR (2010) Complex networks as a unified framework for descriptive analysis and predictive modeling in climate science. Sta Anal Data Mining 4:497–511. doi:10.1002/sam.10100

Steinhaeuser K, Ganguly AR, Chawla NV (2011) Multivariate and multiscale dependence in the global climate system revealed through complex networks. Clim Dyn. doi:10.1007/s00382-011-1135-9

Tsonis AA, Roebber PJ (2004) The architecture of the climate network. Phys A 333:497–504. doi:101016/jphysa200310045

Tsonis AA, Swanson KL (2008) Topology and predictability of El Nino and La Nina networks. Phys Rev Lett 100(22):228502. doi:101103/PhysRevLett100228502

Tsonis AA, Swanson KL, Roebber PJ (2006) What do networks have to do with climate? Bull Am Meteorol Soc 87:585–595

Tsonis AA, Swanson KL, Kravtsov S (2007) A new dynamical mechanism for major climate shifts. Geophys Res Lett 34:L13705. doi:101029/2007GL030288

Tsonis AA, Swanson KL, Wang GL (2008a) On the role of atmospheric teleconnections in climate. J Climate 21(12):2990–3001. doi:101175/2007JCLI19071

Tsonis AA, Swanson KL, Wang G (2008b) Estimating the clustering coefficient in scale-free networks on lattice with local spatial correlation structure. Phys A 387:5287–5294. doi:101016/jphysa200805048

Wang GL, Tsonis AA (2008) On the variability of ENSO at millennial timescales. Geophys Res Lett 35:L17702. doi:101029/2008GL035092

Wang GL, Tsonis AA (2009) A preliminary investigation on the topology of Chinese climate networks. Chin Phys B 18:5091–5096

Wang GL, Swanson KL, Tsonis AA (2008) The pacemaker of major climate shifts. Geophys Res Lett 36:L07708. doi:101029/2008GL036874

Wang XJ, Gong ZQ, Zhou L, Zhi R (2009) Analysis of the stability of temperature networks part 1—the influence of extreme events. Acta Phys Sin 58:6651–6658

Watts DJ, Strogatz SH (1998) Collective dynamics of 'small-world' networks. Nature 393:440–442

Wu GX, Meng W (1998) Gearing between the Indo-monsoon Circulation and the Pacific-Walker Circulation and the ENSO, part I: data analyses. Chin J Atmos Sci 22:470–480

Xu XL, Qu YQ, Guan S, Jiang YM, He DR (2011) Interconnecting bilayer networks. Europhys Lett 93:68002. doi:101209/0295-5075/93/68002

Yamasaki K, Gozolchiani A, Havlin S (2008) Climate networks around the globe are significantly affected by El Nino. Phys Rev Lett 100 (22):228501. doi:101103/PhysRevLett100228501

Zhou CS, Zemanova L, Zamora G, Hilgetag CC, Kurths J (2006) Hierarchical organization unveiled by functional connectivity in complex brain networks. Phys Rev Lett 97:238103. doi:101103/PhysRevLett97238103

Zhou CS, Zemanova L, Zamora-Lopez G, Hilgetag CC, Kurths J (2007) Structure–function relationship in complex brain networks expressed by hierarchical synchronization. New J Phys 9:178. doi:101088/1367-2630/9/6/178

Zhou L, Gong ZQ, Zhi R, Feng GL (2008) An approach to research the topology of Chinese temperature sequence based on complex network. Acta Phys Sin 57:7380–7389

Zhou L, Gong ZQ, Zhi R, Feng GL (2009) Study on the regional characteristics of the temperature changes in China based on complex network. Acta Phys Sin 58:7351–7358

Zhou L, Zhi R, Feng AX, Gong ZQ (2010) Topological analysis of temperature networks using bipartite graph model. Acta Phys Sin 59:6689–6696

Zou Y, Donges JF, Kurths J (2011) Recent advances in complex climate network analysis. Complex Syst Complex Sci 8:27–38